

Transcriptional pulsing and consequent stochasticity in gene expression

Srividya Iyer-Biswas ^{*†}, F. Hayot [‡] and C. Jayaprakash ^{*}

^{*}Ohio State University Department of Physics, Woodruff Ave, Columbus, OH 43210, and [‡]Mount Sinai School of Medicine Department of Neurology, Levy Place, New York, NY 10029

Transcriptional pulsing has been observed in both prokaryotes and eukaryotes and plays a crucial role in cell to cell variability of protein and mRNA numbers. The issue is how the time constants associated with episodes of transcriptional bursting impact cellular mRNA and protein distributions and reciprocally, to what extent experimentally observed distributions can be attributed to transcriptional pulsing. We address these questions by investigating the exact time-dependent solution of the Master equation for a transcriptional pulsing model of mRNA distributions. We find a plethora of results: we show that, among others, bimodal and long-tailed (power law) distributions occur in the steady state as the rate constants are varied over biologically significant time scales. Since steady state distributions may not be reached experimentally we present results for the time evolution of the distributions. Because cellular behavior is essentially determined by proteins, we investigate the effect of the different mRNA distributions on the corresponding protein distributions. We delineate the regimes of rate constants for which the protein distribution mimics the mRNA distribution and those for which the protein distribution deviates significantly from the mRNA distribution.

stochastic gene expression | transcriptional pulsing | mRNA distribution | protein distribution | bimodal distribution

Introduction

Cell to cell variability in mRNA and protein numbers is now recognized as a major aspect of cellular response to stimuli, a variability which is hidden in cell population studies. The most egregious example of the latter is provided in cases where a graded average response hides the all-or-nothing behavior of

single cells [1, 2, 3]. Variability of cellular response can have many origins, which are generally classified as extrinsic and intrinsic noise or fluctuations[4]. The source of intrinsic fluctuations is the random occurrence of reactions that can lead to variability for genetically identical cells in identical, fixed environments. Extrinsic fluctuations can have multiple origins, such as variations from cell to cell in the number of regulatory molecules, or signaling cascade components, or fluctuations in cytoplasmic and nuclear volumes. Many studies, both experimental and theoretical from bacteria to eukaryotes have been undertaken to disentangle intrinsic and extrinsic fluctuations [4, 5, 6, 7, 8, 9, 10, 11].

Intrinsic fluctuations arise from either noisy transcription or translation or both, the effects of which can be measured in single cell mRNA and protein experiments. The simplest model of protein number distributions is to consider both transcription and translation as Poisson processes [7]. Recent experimental studies of mRNA distributions have shown strong evidence for transcriptional noise beyond what can be described by a simple Poisson process. In particular, transcriptional pulsing, where bursts of transcription alternate with quiescent periods, has been observed in both prokaryotes and eukaryotes.

SIB and CJ performed the research.

SIB, FH and CJ analyzed the data and wrote the paper.

The authors declare that they have no conflicts of interests.

[†]To whom correspondence should be addressed. E-mail:srividya@mps.ohio-state.edu

Raser and O’Shea [5], who studied intrinsic and extrinsic noise in *Saccharomyces cerevisiae*, showed that the noise associated with a particular promoter could be explained in a transcriptional pulsing model and confirmed it by mutational analysis. Transcriptional bursts were recorded in *E. coli* [12] by following mRNA production in time, and their statistics computed. Evidence for a pulsing model of transcription, obtained from fluorescent microscopy, has also been presented for the expression of the discoidin Ia gene of *Dictyostelium* [13]. Transcriptional bursts have as well been detected in Chinese hamster ovary cells [10]. In these experiments the production of mRNA occurs in a sequence of bursts of transcriptional activity separated by quiescent periods. Transcriptional bursting, an intrinsically random phenomenon, thus becomes an important element to consider when evaluating cell to cell variability. One can predict that in many cases it will be a significant part of overall noise, and most certainly of intrinsic noise. It has been speculated that pulsatile mRNA production might permit “greater flexibility in transcriptional decisions” [13]. Cook et al. [14] have argued that different aspects of haploinsufficiency can be connected to time scales associated with transcriptional bursting.

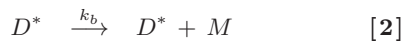
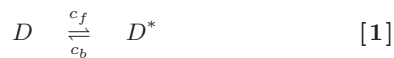
Our study focusses on the consequences of transcriptional bursting in a simplified model of transcription that has been the subject of many studies and is believed to encapsulate the key features of bursting [2, 5, 10, 12, 15, 16]. The complex phenomena that can occur in transcription (chromatin remodeling, enhanceosome formation, preinitiation assembly, etc.) are modeled through positing two states of gene activity: an inactive state where no transcription occurs, and an active one, in which transcription occurs according to a Poisson process. The production of mRNA is thus pulsatile: temporally there are periods of inactivity interspersed with periods or bursts of transcriptional activity. Qualitative features of this model were presented in reference [2], and as-

pects of it relating to bursts explored and discussed in reference [12]. Raj et al. [10] provided a steady state solution to the Master Equation of the transcriptional model considered here, and analyzed it for some ranges of the rate constants. Given the range of time scales that can occur in transcriptional processes in different organisms, it is imperative to highlight the most significant behaviors that can arise in this model and investigate how these depend on the many time scales. In this paper, we provide a comprehensive analysis of a transcriptional pulsing model with an exact solution to the *time-dependent* Master Equation for mRNA production. The advantage of this model is that it is amenable to such an analytic determination of the probability distribution of mRNA copy number as a function of time. We find that the system exhibits a surprising variety of distributions of mRNA number: this includes a bimodal distribution with power-law behavior between the peaks that evolves into a scale-invariant power-law distribution as we vary the rates of activation and inactivation. In some systems the mRNA distribution may not reach steady state, and it is therefore necessary to determine the time evolution of the distributions and characterize the time scales over which steady state is attained. Our time-dependent analytic solution allows us to address these issues in detail, revealing in particular that the mRNA lifetime plays a key role in shaping the mRNA distribution. Cellular behavior is however determined by proteins and not the corresponding mRNA. Therefore, an important question is to what extent the protein distributions follow the mRNA distributions obtained as a result of transcriptional pulsing. To answer this question, we have performed numerical simulations of a model using the Gillespie algorithm [17] in which proteins are produced in a birth-death process from mRNA. When the protein decay rates are much larger than the mRNA decay rate the protein distributions reflect the mRNA distributions; when the protein de-

cays more slowly the protein distribution can be very different from that of the parent mRNA, even in the steady state. We delve deeply into the structure of the transcriptional bursting model, highlighting how the shapes of mRNA distributions depend on the ratios of time scales, determining over which time scales distributions evolve to steady state, and stressing the importance of considering the full distribution rather than characterizing it solely by its average and variance. We thus provide an overview of possible behaviors which yield a framework for interpreting experimental results on transcriptional bursting across prokaryotes and eukaryotes.

Results

We study a model of transcriptional pulsing described by the following reactions where D and D^* denote the gene in the inactive and active states respectively:



The first equation describes the switching “on” and “off” of the gene at the rates c_f and c_b respectively. The second and third equations describe transcription of the mRNA at a constant rate k_b in the active state and the subsequent degradation of the mRNA at a rate k_d . We present results for $P(m, t)$, the probability for the cell to contain m mRNA molecules at a time t that describes cell-to-cell variability of mRNA copy number as a function of time.

Time scales. The steady state and temporal behaviors of the mRNA distribution depend on the rate constants that control the time scales of various processes. Therefore, we begin by briefly summarizing the different time scales that arise in the model. The model has four rate constants, the forward and backward rates for the gene to switch between the active and inactive states and the transcription and degradation rates that govern mRNA numbers, lead-

ing to three independent, dimensionless ratios. The equation obeyed by the probability for the DNA to be in the excited state, denoted by $Q_1(t)$ can be obtained directly from Equation (1): $dQ_1/dt = c_f - (c_f + c_b)Q_1$. This shows that the effective DNA relaxation rate to the steady state is governed by $c_f + c_b$. The mean mRNA number obeys the equation $d\langle m(t) \rangle/dt = -k_d\langle m \rangle + k_bQ_1(t)$. It is thus clear that the temporal behavior of the mean mRNA number is determined by the rates k_d and $c_f + c_b$, the latter entering since it determines the dynamics of the transcriptionally active state. As long as $k_d < c_f + c_b$, the mRNA decay rate sets the time scale over which relaxation to the steady state occurs. We find that the results of our exact solution can be interpreted in the most natural and transparent way when we measure time in units of k_d^{-1} , i.e. in terms of the mRNA lifetime. Thus we will use the three dimensionless ratios k_b/k_d , c_f/k_d , and c_b/k_d to organize our results. The mean number of mRNA in the steady state is given by the product of $c_f/(c_f + c_b)$, the fraction of the time the gene is in the activated state and k_b/k_d , the mean value of mRNA if the gene is always ‘on’. The ratio k_b/k_d clearly sets the scale for the number of mRNA and increasing it extends the range over which $P(m)$ is appreciable without a significant change of shape. The remaining ratios c_f/k_d and c_b/k_d determine the shape of the distribution.

Superposition of Poisson distributions. We begin by providing an intuitively appealing way to view our exact result for $P(m, t)$. The key conclusion is that $P(m, t)$ can be pictured as a superposition of Poisson distributions with different mean values. If the gene is always “on” the mRNA distribution in steady state is Poisson with the Poisson parameter, λ , given by the mean k_b/k_d , the ratio of transcription and degradation rates. Since the gene flips between the “on” and “off” states with the rates determined by c_f and c_b , the mRNA distribution is determined by a stochas-

tic transcription rate $k_b\zeta(t)$ where $\zeta(t)$ is a dichotomous noise that assumes values 0 or 1 corresponding to the gene being in the inactive or active state respectively. The dynamics of the random variable ζ is determined by the stochastic chemical reaction described by Equations (1). Thus the distribution of the mRNA number is described by a Poisson process in which the parameter λ itself is stochastic, a process called a doubly stochastic Poisson process [18].

Consider observing a particular cell at a time T . The number of mRNA at time T is distributed according to a Poisson distribution with parameter $\lambda(T)$ that depends on the time history of $\zeta(t)$ from 0 to T describing the sequence of flips between the on and off states in that cell. This time history corresponds to a series of pulses of unit height with both the widths of the pulses and the intervals between pulses independently and exponentially distributed with parameters c_f and c_b respectively. Different cellular behaviors correspond to different realizations of the random sequence of pulses. Thus cell to cell variability in mRNA copy number is given by a superposition of Poisson distributions with parameter λ that is itself a random variable:

$$P(m, t) = \int d\lambda \rho(\lambda, t) e^{-\lambda} \frac{\lambda^m}{m!} \quad [4]$$

where $\rho(\lambda, t)$ is the probability density of the random variable λ . The fraction of cells with m copies of mRNA at time t is determined by $\rho(\lambda, t)$. Such superpositions have been considered in the context of stochastic processes, for example, in [19]. This representation provides an attractive conceptual framework for understanding the transcriptional pulsing problem. We shall elaborate elsewhere on how the different forms of $\rho(\lambda, t)$ in the different regions of parameter space allow us to interpret the corresponding behaviors of $P(m, t)$.

Steady state distributions. We now describe the variety of steady state distributions that occur in different regions of parameter space. In view of the discussion of time scales in the previous section, it is natu-

ral to classify the distributions by plotting c_f/k_d and c_b/k_d along the x - and y -axes for fixed k_b/k_d . The results for fixed value $k_b/k_d = 100$ are displayed in Figure 1 and provide a bird's eye view of the strikingly different mRNA distributions that arise in different regions of parameter space. We recall that the experiments are performed on a variety of organisms both prokaryotic and eukaryotic. While rate constants are not known, given the different time scales involved in the experiments, we have chosen to investigate a range of values of c_f/k_d and c_b/k_d that encompass different biologically significant cases: for example, our choices include the vastly different rate constant values in the experiments of Raser and O'Shea [5] and Raj et al. [10].

We start with the interesting case displayed in the bottom left figure in Figure 1, when the mRNA half-life is shorter than the time scales over which the gene turns on or off, i.e., $c_f, c_b < k_d$. In the steady state at any given time, the gene is off in some cells. Since the mean duration of the pulse $1/c_b > 1/k_d$ the transcripts produced in the previous occurrence of the on state would probably have decayed and so the number of transcripts will usually be small in these cells. This causes a peak in the mRNA distribution near $m = 0$. In those cells in which the gene is on at the time of observation the number of transcripts can display a broad range of values depending on how long the gene was active as compared to the mRNA lifetime. Thus, we expect to observe a bimodal distribution, as was qualitatively argued in [2]. The result is shown in the lower left quadrant of Figure 1. One finds a peak at $m = 0$ (with a weight that can be computed analytically) and another peak at large ($\sim k_b/k_d$) m values. If the values of c_f and c_b are such that the peaks are well-separated, much of the intermediate region displays a power-law behavior. This reflects the broad range of times for which the gene has been active in different cells at the time of observation. It is useful to remark that bimodal

distributions have been obtained in models with feedback [20]. In contrast, in the transcriptional pulsing model bimodality is obtained *without* the presence of a feedback loop.

Now imagine that we keep c_f fixed and vary c_b so that it is larger than the decay rate. This leads to a scale-invariant, power-law behavior over a significant range of mRNA values. This simple power-law decay obtained in the case $c_f < k_d$ and $c_b > k_d$ is illustrated in the lower right quadrant of Figure 1. This case has been treated analytically in [15, 10]. The mRNA distribution can be fitted by a Gamma distribution, which for appropriate values of the rate constants, shows power-law behavior over a substantial range.

When both the activation and inactivation rates are rapid, i.e., $c_f, c_b \gg k_d$, eliminating the fast reactions naively yields a simple birth-death process for the mRNA with an effective transcription rate $k_b \times c_f / (c_f + c_b)$. This would lead one to expect a Poisson distribution for the mRNA number. However, in this ‘quadrant’, i.e. for $c_f, c_b > k_d$, the observed distribution has a broad single-humped shape as displayed in the upper right quadrant of Figure 1, much broader than a Poisson distribution. This broadening occurs because the parameter λ itself is stochastic. When $c_f > k_d > c_b$ the gene is on most of the time. Not surprisingly, the distribution is Poisson to a very good approximation as seen in the upper left quadrant of Figure 1. In the intermediate region when $c_f, c_b \sim k_d$ the distribution interpolates between these different possibilities and is rectangular when they are equal (see Figure 1, center).

Time evolution of probability distributions. Because of the range of possible time scales, it can happen that the time when measurements are made, the biological system has not attained steady state. For this reason, we now present results for how the distributions evolve to a steady state from an ini-

tial state with no mRNA and the gene in its inactive state. Using the time-dependent result for the distribution (see Material and Methods, equation (9)), we evaluate the evolution using *Mathematica* and plot the complete probability distribution as a function of time. Consider the case $c_f, c_b < k_d$, (bottom left in Figure 1), where the mRNA distribution displays bimodality. Here the mRNA decay rate sets the scale for approach to the steady state. Figure 2(a) shows the evolution of the bimodal distribution as a function of time. For the given initial condition the second peak away from zero develops after a period of roughly twice the mRNA half-life. Steady state behavior sets in at about 4 to 5 times k_d^{-1} . It is clearly possible that, depending on the relative values of the cell cycle time and the mRNA half-life, steady state and therefore, full bimodality may not be observable.

Consider now the time evolution of the distribution that evolves into the ‘pure’ power law behavior featured in the bottom right of Figure 1. In Figure 2(b) we plot $P(m, t)$ vs m on a double logarithmic plot. We have chosen $c_f = 0.25k_d$ and $c_b = 2.5k_d$ to illustrate this case. Larger values of the transcription rate will lead to a larger range over which the power law behavior obtains. It is clear that the exponent of the power law increases in magnitude with time and saturates at the steady state value for t greater than about $4k_d^{-1}$. Thus the shape the distribution depends crucially on the time (measured in units of the decay time) when experimental measurements are made.

Mean and variance versus full distribution. From the examples given in Figure 1 it is clear that the complete probability distribution of mRNA number is required to characterize the behavior of the transcriptional pulsing model. Nevertheless, for completeness, we make some remarks concerning attempts to represent a mRNA distribution by its mean and variance only.

We recall the expressions for the mean and variance in mRNA number in the transcriptional puls-

ing model reported in [5]. The mean is given by $\mu = k_b c_f / (k_d (c_f + c_b))$ and the variance by

$$\sigma^2 = \frac{k_b}{k_d} \frac{c_f}{c_f + c_b} \left(1 + \frac{k_b c_b}{(c_f + c_b)(k_d + c_f + c_b)} \right) \quad [5]$$

The first term in (5) is equal to the mean while the second term arises from the stochasticity in the pulsing process. It can be shown [18] that

$$\sigma^2 = \langle \lambda \rangle + \sigma_\lambda^2 \quad [6]$$

Thus, in a doubly stochastic birth-death process the variance in mRNA number has an additional contribution due to the stochasticity of gene activation and inactivation.

There are two popular measures of noise in terms of the first two moments of a probability distribution: the coefficient of noise, ξ , defined as the ratio of the standard deviation σ to the mean μ , and the noise strength or Fano factor, η , defined as the ratio of the variance σ^2 to the mean. The latter has the value of unity for a Poisson distribution and is therefore convenient for describing deviations from Poisson behavior. In Figure 3 we display constant η contours as a function of c_f/k_d and c_b/k_d for a fixed value of k_b/k_d on a logarithmic scale to encompass a broad range of parameter variation. When $c_f < k_d$ and $c_b > k_d$, the steady state distribution $P(m)$ is monotonically decreasing and has a power law region. In this region, to a first approximation η is independent of c_f (and $\approx 1 + k_b/(k_d + c_b)$) and the contours are roughly parallel to the c_f axis. This emphasizes the possibility that σ^2/μ is a constant for systems with power-law behavior in which c_f varies over a broad range of values. Since as we show later, the protein distribution can reflect the behavior of the corresponding mRNA distribution, the protein distribution can show a similar constancy of the Fano factor. Such a behavior has been observed experimentally in [21] where a pulsing model was discussed. In the region where $c_f, c_b < k_d$, then $\eta \approx 1 + (k_b/k_d)/(1 + c_f/c_b)$ and thus depends only on c_f/c_b . This is consistent with the contours in

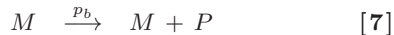
this region being straight lines with slope 1. For the region with $c_f, c_b > k_d$, there is rapid switching between on and off states and the Fano factor depends weakly on the rates c_f and c_b .

There is danger in characterizing distributions solely by their mean and variance. The variety of possible mRNA distributions across cells shown in Figure 1, demonstrates this. One of the interesting results in Reference [5] showed the decrease in the noise strength (Fano Factor) with increase in the mean for genes with different activation rates. Here we show that a wide variety of distributions underlies this correlation between the noise strength and the mean. The increase in the mean can be obtained in the model through an increase in the activating rate, namely the rate c_f , and experimentally through mutations of an appropriate promoter [5]. Even though a smooth curve is obtained for the decrease of noise strength with the mean, we illustrate how the full mRNA distribution can differ for different points along the curve. For specificity, we choose parameter values $k_b = 200k_d$ and $c_b = k_d$, and vary the forward rate c_f for gene activation which changes the mean value. The result is shown in Figure 4(a) and is similar to that obtained experimentally. Now we examine the full probability distribution at three values of c_f , namely $c_f = 0.1k_d$, k_d , and $10k_d$, which correspond to mean values of 18, 100, and 181 respectively. The mRNA distributions are shown in Figure 4(b): the distribution ranges from power-law decay of $P(m)$ for $c_f = 0.1k_d$ to a broadened Poisson distribution for $c_f = 10k_d$. Furthermore, as we pointed out earlier, the value of mRNA degradation rate plays an important role in determining the type of mRNA distribution, a role not apparent in the regimes discussed in [5].

Since we have an analytic expression for the complete distribution we can use an information-theoretic characterization of the mRNA probability distribution, the Shannon entropy. We evaluate the Shan-

non entropy for different values of the rate constants. While the flat distribution clearly corresponds to high entropy, the power-law distribution also yields large values of the entropy indicating that greater information content than the other distributions. The results are presented in Supplementary Section B.

Protein distributions. Given the variety of mRNA distributions that can result from genes undergoing transcriptional pulsing, it is important to understand how this affects the probability distributions for the corresponding protein. While a careful answer to this question would require detailed modeling of mRNA translocation and translation, we address this issue in a model in which translation is treated as a Poisson process [7]. Thus, we use



The effective protein degradation rate would include contributions from cell division, dimerization and other gene specific processes involving the loss of proteins. From our results we identify two regimes, one in which the protein distribution is similar to the mRNA distribution and another in which they are different.

The protein distribution qualitatively mirrors the mRNA distribution if the protein dynamics is faster than the mRNA dynamics: translation and protein degradation occur at a rate higher than the mRNA degradation rate k_d (with $c_f + c_b$ of the order of k_d). In this case, bimodals give rise to bimodals, power-laws give rise to power-laws and so on. The results are displayed in Figure 5, where the protein distributions for two of the cases illustrated in Figure 1 are shown along with the corresponding mRNA distributions. We show results for the protein degradation rate p_d set to twice k_d , the mRNA degradation rate. Figure 5(a) has rate constants c_f, c_b such that the mRNA distribution exhibits bimodality, as seen in the inset. The protein distribution is also clearly bi-

modal for this case. Similarly, in Figure 5(b), a long tailed mRNA distribution with a power law region gives rise to a similar protein distribution when the other rate constants are appropriately chosen.

The other important case is when the proteins are relatively stable compared to the mRNA. This case is more complex; however, there are ranges of rate constants for which the protein and mRNA distributions are vastly different. We illustrate this with two examples. If the rate constants are chosen such that the mRNA distribution is bimodal (cf. Figure 1), then $P(p)$ is qualitatively different from $P(m)$ if $p_d < c_f + c_b$. The protein distributions for this case may be either monotonically decreasing or bell-shaped, depending on whether p_d is less than one or both of c_f, c_b . This contrast between the protein and the mRNA distributions is illustrated in Figure 6(a). A second case is displayed in Figure 6(b) for values of the rate constants that lead to a power-law distribution for the mRNA. Here a bell-shaped distribution is obtained for $P(p)$ when $p_d \ll c_f < k_d < c_b$. These examples demonstrate that one has to be careful in inferring the shape of one of the mRNA or protein distributions from the other.

It is worth noting that even if mRNA numbers are small, even as low as $\mathcal{O}(10)$, the above conclusions continue to hold. Thus, a wide variety of protein distributions that may or may not reflect the underlying mRNA distribution could be realized in real biological systems when the gene undergoes transcriptional pulsing.

It has been argued recently [22] that if the effective protein degradation is very slow compared to that of the mRNA, the protein distribution can be approximated by a gamma distribution. While gamma distributions do provide a good fit for some regions of parameter space, none of the distributions obtained in the bimodal quadrant can be reasonably approximated by a gamma distribution.

Discussion

In this paper, we have presented results for the time-dependent and steady-state probability distributions for mRNA in a transcriptional pulsing model. A variety of mRNA distributions occur in different regimes of rate constants. Our aim is to provide a guide for the interpretation of data on cell-to-cell variability that could arise from transcriptional pulsing. Transcriptional pulsing, entailed by the dynamics of chromatin remodeling, reinitiation and similar processes, appears as a straightforward mechanism leading to bimodality and also to mRNA distributions with long tails. Long-tailed distributions of mRNA have been seen in a variety of systems: the experiments of Raser and O’Shea [5] show evidence for long tails which they attribute to transcriptional pulsing. In experiments on the gene ActB in cells from mouse pancreatic islets the distribution of mRNA number, m , was found to be consistent with a log-normal distribution that would correspond to $P(m) \sim m^{-1}$ over some range of m [23]. More recently, a similar distribution of the Interferon- β gene transcripts has been found in human dendritic cells [11]. For the latter two experiments our results should help clarify whether the origin of the mRNA behavior lies in transcriptional pulsing. However, cell behavior is controlled not by mRNA but by the proteins they encode. Therefore, it is crucial to determine whether the protein distribution follows the corresponding mRNA distribution. We have determined when the two distributions are similar but also identified situations when the protein distributions are strikingly different from those of the mRNA. In general, and for these situations in particular, our results on the range of cell-to-cell variability of mRNA and protein responses due to transcriptional pulsing should provide significant help in interpreting experiments.

Materials and Methods

The results presented and discussed here for mRNA are based on the exact form of the distribution function $P(m, t)$ of the mRNA number, m at time t . We have solved the Master Equation [19] for reactions (1)-(3) that describes the time evolution of the distribution to obtain these results. We found it convenient to work with the generating function defined by $G(z, t) = \sum_{m=0}^{\infty} z^m P(m, t)$. If we can evaluate $G(z, t)$ exactly, then the probability of having m mRNA transcripts at time t can be obtained by extracting the coefficient of the z^m term. We have computed the generating function exactly (See Supplementary Section A for the details) for the initial condition with zero mRNA, i.e., $P(m, 0) = \delta_{m,0}$, and find

$$G(z, t) = F_s(t)\Phi(c_f, c_f + c_b; -k_b(1 - z)) + F_{ns}(t)(1 - z)\Phi(1 - c_b, 2 - c_f - c_b; -k_b(1 - z)) \quad [9]$$

where Φ is the (Kummer) confluent hypergeometric function [24, 25] and the coefficients $F_s(t)$ and $F_{ns}(t)$ can be calculated explicitly in terms of confluent hypergeometric functions. The results are displayed in Supplementary Section A. At large times $F_s = 1$ and $F_{ns} = 0$. Thus in the steady state the generating function is given by (see also [10])

$$G_s(z) = \Phi(c_f, c_f + c_b; -k_b(1 - z)), \quad [10]$$

We can use the exact solution in Equation (9) to extract the *time-dependent* behavior of $P(m, t)$ or Equation (10) for the steady state for different ranges of values of the rate constants. The results presented were obtained by extracting the coefficients of z^m in the expansion of the generating function using *Mathematica*[26]. While standard numerical simulations based on the Gillespie algorithm [17] can be employed to study both the steady state and the time evolution, the exact solution allows us to extract the results much more efficiently and explore the behavior of the system systematically in the space of rate constants

without statistical errors, especially, when there are long tails present. The results for the protein distributions were obtained from numerical simulations using the Gillespie algorithm.

This work was supported by the National Institute

of Allergy and Infectious Diseases through contract HHSN266200500021C. We thank Stuart Sealfon, James Wetmur, and Jianzhong Hu for discussions that stimulated this work and Stuart Sealfon for a careful reading of the manuscript and comments. S. I. B. thanks Rudro R. Biswas for productive discussions.

1. Fiering S, Northrop JP, Nolan GP, Mattila PS, Crabtree GR, Herzenberg LA (1990) Single cell assay of a transcription factor reveals a threshold in transcription activated by signals emanating from the T-cell antigen receptor. *Genes & Development* 4:1823-1834.
2. Hume DA (2000) Probability in transcriptional regulation and its implications for leukocyte differentiation and inducible gene expression. *Blood* 96:2323-2328.
3. Ko MS (1992) Induction mechanism of a single gene molecule: stochastic or deterministic? *Bioessays* 14:341-346.
4. Elowitz MB, Levine AJ, Siggia ED, Swain PS (2002) Stochastic gene expression in a single cell. *Science* 297:1183-1186; Swain PS, Elowitz MB, Siggia ED (2002) Intrinsic and extrinsic contributions to stochasticity in gene expression. *Proc Natl Acad Sci USA* 99:12795-12800.
5. Raser JM, O'Shea EK (2004) Control of stochasticity in eukaryotic gene expression. *Science* 304:1811-1814.
6. Blake WJ, Kaern M, Cantor CR, Collins JJ (2003) Noise in eukaryotic gene expression. *Nature* 422:633-637.
7. Thattai M, van Oudenaarden A (2001) Intrinsic noise in gene regulatory networks. *Proc Natl Acad Sci USA* 98:8614-8619.
8. Ozbudak EM, Thattai M, Kurtser I, Grossman AD, van Oudenaarden A (2002) Regulation of noise in the expression of a single gene. *Nat Genet* 31: 69-73.
9. Paulsson J (2004) Summing up the noise in gene networks. *Nature* 427:415-418
10. Raj A, Peskin CS, Tranchina D, Vargas DY, Tyagi S (2006) Stochastic mRNA synthesis in mammalian cells. *PLoS Biology* 4:1707-1719
11. Hu J, Sealfon SC, Hayot F, Jayaprakash C, Kumar M, Pendleton AC, Ganee A, Fernandez-Sesma A, Moran TM, Wetmur JG (2007) *Nucleic Acids Res* doi:10.1093/nar/gkm557
12. Golding I, Paulsson J, Zawilski SM, Cox EC (2005) Real-time kinetics of gene activity in individual bacteria. *Cell* 123:1025-1036.
13. Chubb J, Trcek T, Shenoy S, Singer R (2006) Transcriptional pulsing of a developmental gene. *Current Biology* 16:1018-1025.
14. Cook DL, Gerber AN, Tapscott SJ (1998) Modeling stochastic gene expression: Implications for haploinsufficiency. *Proc Natl Acad Sci USA* 95:15641-15646
15. Karmakar R, Bose I (2006) Graded and binary responses in stochastic gene expression. *Physical Biology* 1:197-204
16. Kepler TB, Elston TC (2001) Stochasticity in transcriptional regulation: origins, consequences, and mathematical representations. *Biophys J* 81:3116-3136
17. Gillespie DT (2001) Exact stochastic simulation of coupled chemical reactions. *J Chem Phys* 115:1716-1733.
18. Cox DR, Isham V (1980) in *Point Processes* (Chapman and Hall, London)
19. Gardiner CW (1997) *Handbook of Stochastic Methods* (Springer Berlin)
20. Ferrell JE (2002) Self-perpetuating states in signal transduction: positive feedback, double-negative feedback and bistability. *Curr. Opin. Cell Biol.* 14:140-148.
21. Bar-Even A, Paulsson J, Maheshri N, Carmi M, O'Shea E, Pilpel Y, and Barkai N (2006) Noise in protein expression scales with natural protein abundance. *Nat Genet* 38:636-643.
22. Friedman N, Cai L Xie SX (2006) Linking stochastic dynamics to population distribution: an analytical framework of gene expression. *Phys Rev Lett* 97:168302.
23. Bengtsson M, Ståhlberg A, Rorsman P, Kubista M (2005) Gene expression profiling in single cells from the pancreatic islets of Langerhans reveals lognormal distribution of mRNA levels. *Genome Res* 15: 1388-1392.
24. Abramowitz M, Stegun IA (1964) *Handbook of Mathematical Functions* (US Govt. Printing, Wahington DC)
25. Slater LJ (1960) in *Confluent Hypergeometric Functions* (Cambridge, England)
26. Wolfram Research, Inc.,(2005) *Mathematica*, Version 5.2, Champaign, IL

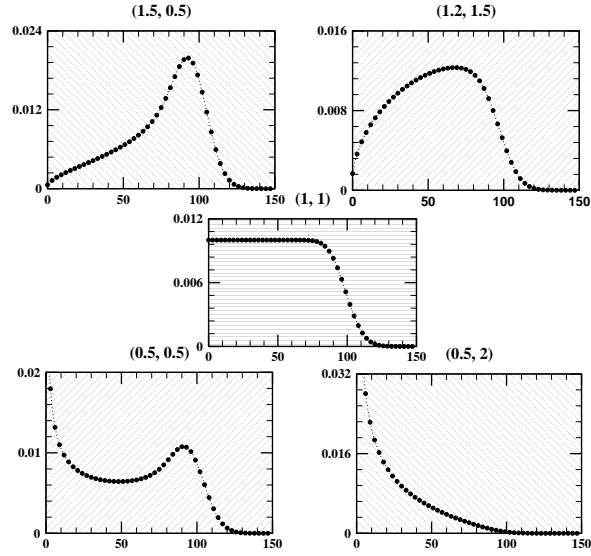


Fig. 1. Steady state mRNA distributions $P(m)$ vs. m , labeled by (c_f, c_b) in units of k_d . The mRNA transcription rate k_b is $100k_d$ for all the distributions. The figure shows prototype distributions for the five major regimes $c_f, c_b \leq k_d$ in parameter space. The distribution for $c_f, c_b = k_d$ is flat. Bimodals are obtained in the lower left panel for $c_f, c_b < k_d$ while a power law occurs in the lower right panel.

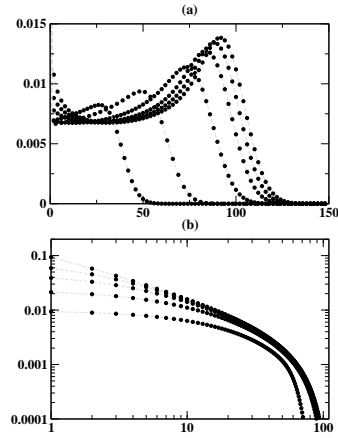


Fig. 2. Time evolution of $P(m, t)$ towards steady state as a function of m at different time points (a) in the bimodal regime for $c_f = 0.75k_d$, $c_b = 0.5k_d$ and $k_b = 100k_d$ at times $t = 0.5, 1, 2, 3, 4$ and ∞ in units of k_d^{-1} . The steady state with bimodality is reached around $4k_d^{-1}$. (b) Log-Log plot of $P(m, t)$ for $c_f = 0.25k_d$, $c_b = 2.5k_d$ and $k_b = 100k_d$ at times $t = 1, 2, 3, 4$ and ∞ in units of k_d^{-1} . The figure shows the time evolution of the power law region of $P(m, t)$. For the different curves time increases from bottom to top with the slope increasing to its steady-state value.

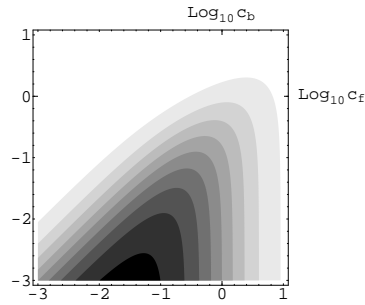


Fig. 3. Contour plot of the noise strength(Fano factor) η as c_b and c_f (in units of k_d) are varied, for $k_b = 1000k_d$, in the steady state; c_b and c_f are varied on a \log_{10} scale over 5 decades. 9 contours for different values of η are placed at intervals of 100, from 1 to 1001 with η increasing from light to dark values.

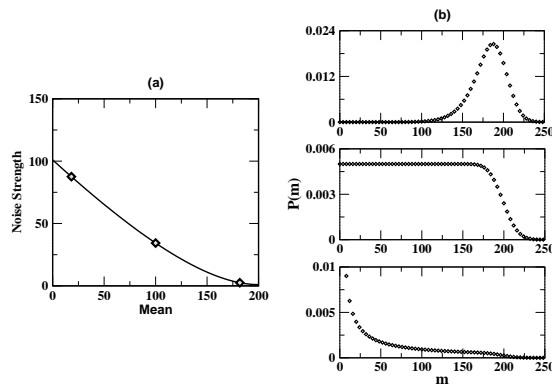


Fig. 4. Smoothly varying noise strengths as activation rate is varied can correspond to different probability distributions. (a) Variation of noise strength (Fano factor) with activation rate for $k_b = 200k_d$ and $c_b = k_d$ (b) The steady state distributions $P(m)$ corresponding to the (diamond-shaped) points marked in (a). The points in (a) going from right to left and the corresponding figures from top to bottom in (b) are for $c_f/k_d = 10, 1,$ and 0.1 respectively. Figure (b) illustrates how different points on the same curve (a) can be associated with dramatically different mRNA distributions.

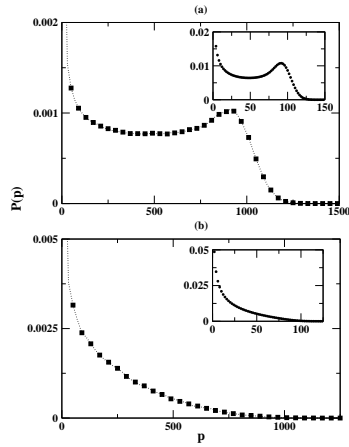


Fig. 5. Examples of steady state distributions of proteins reflecting those of mRNA. Protein distributions (a) for $c_f = 0.5k_d$, $c_b = 0.5k_d$ and $k_b = 100k_d$, $p_b = 20k_d$ and $p_d = 2k_d$ (b) for $c_f = 0.5k_d$, $c_b = 2k_d$ and $k_b = 100k_d$, $p_b = 20k_d$ and $p_d = 2k_d$. The insets show the corresponding mRNA distributions. When the protein degrades faster than the mRNA, its distribution qualitatively mirrors the corresponding mRNA distribution.

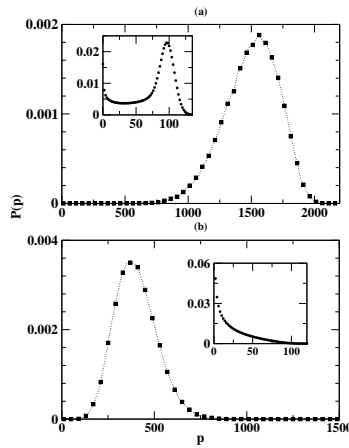


Fig. 6. Examples of steady state distribution of proteins differing from those of mRNA. Protein distributions for (a) for $c_f = 0.6k_d$, $c_b = 0.2k_d$ and $k_b = 100k_d$, $p_b = 1k_d$ and $p_d = 0.05k_d$ (b) for $c_f = 0.5k_d$, $c_b = 2k_d$ and $k_b = 100k_d$, $p_b = 1k_d$. The protein lifetime is 20 times longer than the mRNA lifetime. The insets show the corresponding mRNA distributions. When the protein degrades slowly compared to the mRNA, its distribution can be qualitatively different from the corresponding mRNA distribution.

Supplementary Section A

Time-dependent solution to the Master Equation for transcriptional bursts

For the set of reactions described by Equations 1-3 in the text we define $P_0(m, t)$ and $P_1(m, t)$ to be the probability that at time t the cell has m mRNA molecules and the gene is in the inactive and active states respectively. It is straightforward to write down the Master Equation for the two probabilities:

$$\frac{dP_0(m, t)}{dt} = -c_f P_0(m, t) + c_b P_1(m, t) + k_d [(m+1)P_0(m+1, t) - mP_0(m, t)] \quad (1)$$

$$\begin{aligned} \frac{dP_1(m, t)}{dt} = & c_f P_0(m, t) - c_b P_1(m, t) + k_d [(m+1)P_1(m+1, t) - mP_1(m, t)] \\ & + k_b [P_1(m-1, t) - P_1(m, t)] \end{aligned} \quad (2)$$

We define the generating functions

$$G_\alpha(z, t) \equiv \sum_{m=0}^{\infty} z^m P_\alpha(m, t)$$

for $\alpha = 0$ and 1 . The mRNA distribution (independent of the state of the gene) is determined by the sum $G \equiv G_0 + G_1$. It is easy to deduce the equations obeyed by the generating functions from the Master Equations (with time re-scaled by k_d):

$$\partial_t G_0(z, t) = -c_f G_0(z, t) + c_b G_1(z, t) + (1-z) \partial_z G_0(z, t) \quad (3)$$

$$\partial_t G_1(z, t) = c_f G_0(z, t) - c_b G_1(z, t) + (1-z) \partial_z G_1(z, t) - k_b(1-z)G_1(z, t). \quad (4)$$

All the rate constants are measured in units of k_d .

We simplify the equations using an analog of the Galilean transformation by making the change of variables $v \equiv k_b(1-z)$ and $w \equiv ve^{-t} = k_b(1-z)e^{-t}$. In terms of the transformed variables, we have

$$v\partial_v G_0 = -c_f G_0 + c_b G_1 \quad (5)$$

$$v\partial_v G_1 = c_f G_0 - c_b G_1 - vG_1. \quad (6)$$

Adding the two equations we have the useful relation

$$\partial_v (G_0 + G_1) = -G_1. \quad (7)$$

Note that $G_0(z, t)$ and $G_1(z, t)$ (and hence, their sum) are functions of v only and independent of $w = k_b(1-z)e^{-t}$; the dependence on w is determined by the boundary conditions.

It is convenient to derive a second-order differential equation for G . Therefore we differentiate the equations for G_0 and G_1 and obtain (7)

$$v\partial_v^2 G_0 + (1 + c_f + c_b + v)\partial_v G_0 + c_f G_0 = 0 \quad (8)$$

$$v\partial_v^2 G_1 + (1 + c_f + c_b + v)\partial_v G_1 + (1 + c_f)G_1 = 0. \quad (9)$$

We add the two equations and use Equation (7) to obtain

$$v\partial_v^2 G + (c_f + c_b + v)\partial_v G + c_f G = 0.$$

The substitution $G(v) = e^{-v}F(v)$ shows that $F(v)$ satisfies the confluent hypergeometric equation in the canonical form. The solution is given by

$$F = A(w)\Phi(c_b, c_f + c_b; v) + B_0(w)v^{1-c_f-c_b}\Phi(1-c_f, 2-c_f-c_b; v). \quad (10)$$

Upon using the Kummer transformation, $e^{-v}\Phi(\alpha, \gamma; v) = \Phi(\gamma - \alpha, \gamma; -v)$, we obtain

$$G = A(w)\Phi(c_f, c_f + c_b; -v) + B_0(w)v^{1-c_f-c_b}\Phi(1-c_b, 2-c_f-c_b; -v). \quad (11)$$

In order to obtain a well-defined power series in $v = k_b(1-z)$ for the generating function we must impose

$$B_0(w) = w^{c_f+c_b}B(w) = v^{c_f+c_b}e^{-(c_f+c_b)t}B(w).$$

This yields the form

$$G = A(w)\Phi(c_f, c_f + c_b; -v) + B(w)e^{-(c_f+c_b)t}v\Phi(1-c_b, 2-c_f-c_b; -v). \quad (12)$$

We impose the boundary conditions at $t = 0$ which corresponds to $w = v$. The initial condition $P(m, t = 0) = \delta_{m,0}$ leads to

$$G(w = v, v) = 1. \quad (13)$$

We assume that the gene is initially in the inactive state and thus $G_1(z, t = 0) = 0$. The additional condition that arises from Equation (7) implies

$$\partial_v G(w, v)|_{w=v} = 0. \quad (14)$$

Imposing these conditions we determine the unknown functions A and B_0 . This involves judicious use of the Wronskian identity

$$\Phi(\alpha - \gamma + 1, 1 - \gamma; z)\Phi(\alpha, \gamma; z) - \frac{\alpha}{\gamma(1-\gamma)}z\Phi(\alpha - \gamma + 1, 1 - \gamma; z)\Phi(\alpha + 1, \gamma + 1, z) = e^z \quad (15)$$

that follows from results in Ref. [1] and other identities to found there. The final result is

$$G(z, t) = F_s(t)\Phi(c_f, c_f + c_b; -k_b(1-z)) + F_{ns}(t)(1-z)\Phi(1-c_b, 2-c_f-c_b; -k_b(1-z)). \quad (16)$$

where

$$F_s(t) = \Phi(-c_f, 1 - c_f - c_b; k_b e^{-t}(1-z)) \quad \text{and} \quad (17)$$

$$F_{ns}(t) = -\frac{c_f k_b(1-z)}{(c_f + c_b)(1 - c_f - c_b)}e^{-(c_f+c_b)t}\Phi(c_b, 1 + c_f + c_b; k_b e^{-t}(1-z)). \quad (18)$$

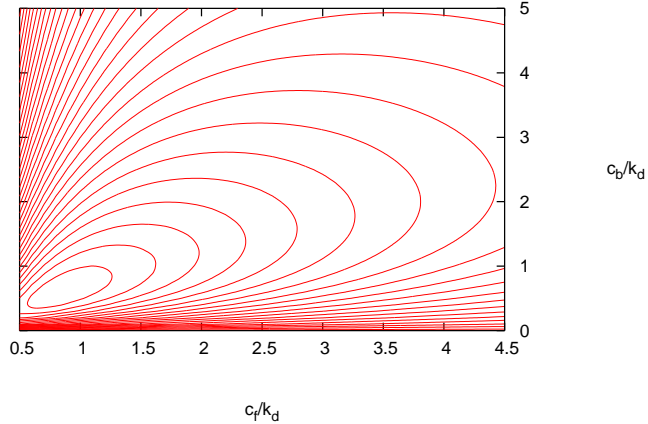


Figure 1: Contour Plot of the Shannon entropy defined in Equation 19 of $P(m)$ for $k_b = 100k_d$; separation between contours is 0.05 and the Shannon entropy decreases outward from the central contour.

Supplementary Section B

Characterization of noise in terms of Shannon Entropy

In information theory the Shannon entropy serves as a measure of the average information content or the uncertainty of a random variable. We now present results for this measure of the noise in the mRNA distribution. Given the exact solution we can directly evaluate the Shannon entropy associated with the steady state distribution $P(m)$ defined by

$$\mathcal{S} = - \sum_i P(m) \log_2 P(m). \quad (19)$$

In Figure 1 we display contours of constant entropy as a function of the forward and backward rates c_f and c_b . Not surprisingly, the values $c_f/k_d, c_b/k_d \simeq 1$ yield the largest entropy since this choice leads to a uniform distribution in $P(m)$. The power law distribution also provides a range of values for the rates in which larger values of entropy can be obtained. Since the Shannon entropy is a measure of the amount of information required to describe the random variable on average it can be helpful in the interpretation of data. For example, consider dendritic cells involved in providing innate immunity to an organism against pathogens. Assume that the mRNA or the protein produced by the cell to overcome a viral antagonist has a broad distribution. It is plausible that the greater the amount of information required to describe the distribution the lesser the chances of the pathogen being able to overcome the

organism's immune system by random mutations. This can confer greater immunity against mutations in the virus that could evade the defence mechanisms of the organism. It is known that the interferon- β mRNA distribution is broad in human dendritic cells [2].

References

- [1] Slater LJ (1960) in *Confluent Hypergeometric Functions* (Cambridge, England)
- [2] Hu J, Sealfon SC, Hayot F, Jayaprakash C, Kumar M, Pendleton AC, Gagnee A, Fernandez-Sesma A, Moran TM, Wetmur JG (2007) *Nucleic Acids Res* doi:10.1093/nar/gkm557